HHS Public Access

Author manuscript

Sci Immunol. Author manuscript; available in PMC 2017 October 23.

Published in final edited form as:

Sci Immunol. 2017 May 12; 2(11): . doi:10.1126/sciimmunol.aam7341.

Virion incorporation of integrin α4β7 facilitates HIV-1 infection and intestinal homing

Christina Guzzo[1,†], **David Ichikawa**[1,†], **Chung Park**[2], **Damilola Phillips**[1,*], **Qingbo Liu**[1], **Peng Zhang**[1], **Alice Kwon**[1], **Huiyi Miao**[1], **Jacky Lu**[1], **Catherine Rehm**[3], **James Arthos**[4], **Claudia Cicala**[4], **Myron S. Cohen**[5], **Anthony S. Fauci**[4], **John H. Kehrl**[2], and **Paolo Lusso**[1,**]

[1]Viral Pathogenesis Section, Laboratory of Immunoregulation, National Institute of Allergy and Infectious Diseases (NIAID), NIH, Bethesda, MD 20892, USA

[2]B-Cell Molecular Immunology Section, Laboratory of Immunoregulation, National Institute of Allergy and Infectious Diseases (NIAID), NIH, Bethesda, MD 20892, USA

[3]Clinical Research Section, Laboratory of Immunoregulation, National Institute of Allergy and Infectious Diseases (NIAID), NIH, Bethesda, MD 20892, USA

[4]Immunopathogenesis Section, Laboratory of Immunoregulation, National Institute of Allergy and Infectious Diseases (NIAID), NIH, Bethesda, MD 20892, USA

[5]Division of Infectious Diseases, Department of Medicine, University of North Carolina at Chapel Hill, Chapel Hill, NC 27599, USA

Abstract

The intestinal mucosa is a key anatomical site for HIV-1 replication and $CD4^+$ T-cell depletion. Accordingly, *in vivo* treatment with an antibody to the gut-homing integrin α4β7 was shown to

**Corresponding author. plusso@niaid.nih.gov.
†These authors contributed equally to this work
*D.P. was a fellow of the NIH Medical Research Scholars from the Cleveland Clinic Lerner College of Medicine, Cleveland, OH

List of Supplementary Materials

Fig. S1. Schematic representation and validation of the immunomagnetic virion-capture assay.
Fig. S2. Role of HIV-1 Gag and Env components in virion incorporation of integrin α4β7.
Fig. S3. Effect of RA treatment on cell-surface expression and virion incorporation of different lymphocyte markers.
Fig. S4. Correlation between α4β7 cell-surface expression and α4β7 incorporation into HIV-1 progeny virions.
Fig. S5. Validation of engineered $\alpha4\beta7^+$ and $\alpha4\beta7^-$ HIV-1 THRO viral stocks.
Fig. S6. Validation of engineered $\alpha4\beta7^+$ and $\alpha4\beta7^-$ HIV-1 BaL pseudovirus stocks.
Video 1. Animation of a three-dimensional image reconstruction showing $\alpha4\beta7^+$ HIV-1 virions captured along the endothelial surface of HEVs in Peyer's patches.
Raw data tables with statistical analyses.

Author contributions:

PL, CG and DI conceived and designed the study; CG, DI, DP, QL, PZ, HM, JL, and AK performed flow cytometry, virus stock production and quantification, virion capture assays, and Western blot analyses; CP and JK performed in vivo homing experiments; MC and CR coordinated clinical samples and patient data collection; JA, CC and ASF provided expert advice on experimental planning and data interpretation; PL and CG performed statistical analyses and wrote the manuscript; all the authors read and commented on the manuscript.

Competing interests:

The authors have no conflicts of interest to declare.

Data and materials availability:

Primary data and statistical analyses are contained in the primary data tables file available online. Materials used in this work are available upon written request to the authors.

reduce viral transmission, delay disease progression, and induce persistent virus control in macaques challenged with SIV. Here, we show that integrin α4β7 is efficiently incorporated into the envelope of HIV-1 virions. Incorporated α4β7 is functionally active as it binds MAdCAM-1, promoting HIV-1 capture by and infection of MAdCAM-expressing cells, which in turn mediate *trans*-infection of bystander cells. Functional α4β7 is present in circulating virions from HIV-infected patients and SIV-infected macaques, with peak levels during the early stages of infection. *In vivo* homing experiments documented selective and specific uptake of $\alpha4\beta7^+$ HIV-1 virions by high endothelial venules in the intestinal mucosa. These results extend the paradigm of tissue homing to a retrovirus and are relevant for the pathogenesis, treatment and prevention of HIV-1 infection.

INTRODUCTION

Although human immunodeficiency virus type-1 (HIV-1) establishes a life-long infection that progresses to overt disease over the course of several years or even decades, the early events of virus-host interaction are critical in determining the pace of disease progression. A key anatomical site for virus replication and pathogenesis during primary HIV-1 infection is the gut-associated lymphoid tissue, which is believed to provide the largest reservoir in the body of $CD4^+$ T lymphocytes, the primary target cells for HIV-1 replication (1–4). Accordingly, the principal gut-homing integrin, α4β7, has been identified as an additional cellular receptor for HIV-1 (5) and is emerging as a critical molecule in the pathogenesis of HIV-1 disease (6). Expression of α4β7 on T cells promotes their trafficking to the gut via interaction with MAdCAM-1, which is expressed at high levels on high endothelial venules (HEV) in the intestinal Peyer's patches, lamina propria and mesenteric lymph nodes (7), as well as on follicular dendritic cells (DCs) in the gut mucosa (8). Intestinal DCs play a critical role in the recruitment and retention of T cells into the gut compartment through the production of retinoic acid (RA), a vitamin A metabolite that induces α4β7 expression, thereby imprinting a gut-homing phenotype on these cells (9, 10).

The role of integrin α4β7 in HIV-1 infection is corroborated by a series of *in vivo* studies in nonhuman primates, which documented a protective role of anti-α4β7 antibodies against challenge with simian immunodeficiency virus (SIV). Intravenous administration of a primatized anti-α4β7 monoclonal antibody (mAb), ACT-1, during acute SIV infection in rhesus macaques was found to markedly decrease plasma and intestinal viral loads, resulting in delayed disease progression (11). Subsequently, the same anti-α4β7 mAb was shown to prevent or delay SIV infection in macaques challenged by repeated low-dose vaginal inoculation (12). Furthermore, administration of anti-α4β7 mAb in the early post-acute phase of infection was recently found to induce persistent control of SIV replication and preservation of the gut lymphoid tissue after withdrawal of antiretroviral therapy (ART) (13). Although these *in vivo* results have provided compelling evidence for the role of α4β7 in SIV transmission and pathogenesis, the precise mechanism(s) of protection afforded by α4β7 blockade remains uncertain.

The extraordinary ability of HIV-1 to persist in the host is due to a unique endowment of virulence factors and immune evasion tactics (14). Among the former, HIV-1 has the

capacity to incorporate a range of host-cell proteins into its external envelope, which may affect its cellular tropism and infectivity (15–17). In particular, virion incorporation of the adhesion molecule CD54/ICAM-1, the natural ligand of CD11a/LFA-1, was previously shown to increase HIV-1 attachment and infectivity (18–21). In the present study, we provide evidence that functional integrin α4β7 is incorporated into the envelope of HIV-1 virions both *in vitro* and *in vivo*, and promotes virus homing to the intestinal Peyer's patches *in vivo* in a mouse model.

RESULTS

HIV-1 virions incorporate integrin α4β7

To assess virion incorporation of host cellular proteins, we utilized a previously described virion-capture assay (22–25) (fig. S1) on HIV-1 progenies produced by peripheral blood mononuclear cells (PBMC) obtained from three unselected blood donors using mAbs against a panel of lymphocyte markers; in parallel, the same mAbs were used to evaluate cell-surface expression of such markers on the homologous HIV-producer cells by flow cytometry (Fig. 1A,B) (25). In line with previous observations (15–17, 26–28), we found that several host-cell proteins were incorporated into HIV-1 virions, including CD11a/LFA-1, CD43, CD54/ICAM-1 and HLA-DR (MHC class II), whereas other proteins, such as CD27 and HLA-ABC (MHC-class-I), were present at very low levels on HIV-1 virions (Fig. 1A). Strikingly, integrin α4β7 was one of the host proteins most efficiently incorporated by HIV-1, as shown by virion capture both with mAbs against the individual integrin subunits (α4 and β7) and with a mAb (ACT-1) specific for the integrin heterodimer (29) (Fig. 1A). When we compared the levels of host protein incorporation into virions (Fig. 1A) with the levels of expression of the same markers on the surface of virus-producing cells (Fig. 1B), it was evident that certain proteins (e.g., α4β7, HLA-DR, CD43) were selectively enriched in virions, while others that were highly expressed on the cellular surface (e.g., CD27, CD45, HLA-ABC) were minimally, if at all, incorporated into virions. To obtain an index of virion-incorporation efficiency, we first normalized the levels of virion incorporation and cell-surface expression to the respective levels detected with ICAM-1, selected as a reference protein; then, for each protein we calculated the ratio between normalized virion incorporation and normalized cell-surface expression. The resulting ratios (Fig. 1C) showed that incorporation of the α4β7 heterodimer was significantly higher than that of ICAM-1 ($p=0.0056$), while the ratio for other proteins, like HLA-DR and CD43, was increased but did not reach statistical significance, most likely due to the wide variability among PBMC from different blood donors. The marked enrichment of selected lymphocyte markers on HIV-1 virions, as opposed to the minimal incorporation of other proteins despite their high expression on the cellular surface, corroborated the concept that virion incorporation does not simply reflect a passive uptake phenomenon correlated with the level of protein expression on the surface membrane of virus-producer cells, but rather a specific mechanism, as suggested for ICAM-1 incorporation (30).

As a first step toward elucidating the mechanism responsible for α4β7 incorporation into HIV-1 virions, we investigated the viral components required for such incorporation. For this purpose, viral pseudoparticles were generated by expression of either the HIV-1 core protein

alone (Gag) or Gag plus the HIV-1 envelope glycoprotein (Env) in the presence or absence of α4β7. When these viral progenies were tested for α4β7 incorporation by virion-capture assays, we found that the presence of Gag alone was sufficient for the viral pseudoparticles to incorporate α4β7, while the addition of Env did not significantly affect the level of α4β7 incorporation (fig. S2), indicating that the Gag protein is sufficient for HIV-1 virions to uptake α4β7 upon budding from the cellular membrane.

Given the central role of the vitamin A metabolite RA in enhancing the cellular expression of α4β7, we investigated whether and to what extent RA treatment affects the level of integrin incorporation by comparing homologous HIV-1 viral progenies produced by cells activated in the presence or absence of RA. Virion-capture assays demonstrated a higher incorporation of α4β7 into viral progenies produced by RA-treated ($\alpha4\beta7^{hi}$) vs. -untreated ($\alpha4\beta7^{lo}$) human PBMC, indicating that the efficiency of incorporation correlates with the level of cell-surface expression of the integrin (Fig. 1D). In contrast, virion incorporation of other lymphocyte markers was not significantly affected by RA treatment (fig. S3). The correlation between the levels of α4β7 cell-surface expression and virion incorporation was further corroborated by titration experiments of α4β7 co-transfected with a full-length HIV-1 molecular clone (THRO) in HEK293 cells (fig. S4).

To obtain a semi-quantitative assessment of the amount of α4β7 protein incorporated into HIV-1 virions, we performed Western blot analyses on concentrated HIV-1 stocks containing equal inputs of $p24_{Gag}$ antigen produced by RA-treated vs. untreated PBMC (Fig. 2). As a reference for quantification, we loaded serial dilutions of recombinant α4β7 (lanes 2–4) and HIV-1 gp120 (lanes 7–9). The cleaved form of the α4 integrin subunit (MW = 70Kd), which is the form typically expressed on the surface of activated T cells (31), was detected in both viral progenies; however, α4 incorporation was higher in virus produced by RA-treated than -untreated PBMC. By densitometric scanning of a representative Western blot, we measured ~600 ng of α4 protein per μ*g* of $p24G_ag$ in virus produced by RA-treated cells vs. ~150 ng in virus produced by untreated cells, while both viral progenies contained similar amounts of HIV-1 gp120Env (~200 ng per μ*g* of $p24_{Gag}$), indicating that in mature HIV-1 virions α4β7 can be present in molar excess of gp120.

α4β7 is incorporated by a wide range of HIV-1 and SIV strains

To evaluate the breadth of incorporation of α4β7 among different clinical and laboratory-adapted HIV-1 strains under canonical virus-propagation conditions, we analyzed a panel of 12 HIV-1 isolates of different coreceptor usage phenotype and genetic subtype, grown exclusively in PHA-activated primary human PBMC in the absence of RA or other co-stimulations (Table 1). Incorporation of α4β7 was detected in all the HIV-1 isolates tested, including both clinical and laboratory-adapted isolates, irrespective of their coreceptor-usage phenotype and genetic subtype; in all the isolates, α4β7 was incorporated more efficiently than ICAM-1/CD54 (Table 1). Additionally, we investigated whether α4β7 can be incorporated by SIV, the simian immunodeficiency retrovirus utilized in nonhuman primate models (11–13). Two different SIV isolates grown in primary human PBMC efficiently incorporated α4β7 into their virions (Table 1).

Virion-incorporated α4β7 is functionally active

The activation state of integrins, which is affected by divalent cations such as manganese (Mn^{++}), influences their ligand binding affinity (32, 33). To determine the functionality of virion-incorporated α4β7, we tested the ability of $\alpha4\beta7^{+}$ HIV-1 virions to bind to the natural integrin ligand, MAdCAM-1, in the presence or absence of various modulators of integrin activation. Magnetic beads were armed with soluble MAdCAM-1, or with mAb ACT-1 as a control, and used to capture HIV-1 virions in the presence or absence of manganese chloride ($MnCl_2$), of the chelating agent EDTA, or of an inhibitory MAdCAM-1 peptide mimetic (ELN) (34). Binding to MAdCAM-1 was detected even in the absence of activating stimuli (Control), indicating that at least a fraction of the incorporated integrin is present in a functionally active state (Fig. 3). Treatment with 1 mM $MnCl_2$, which induces α4β7 to adopt a high-affinity ligand-binding state (32), dramatically increased capture by MAdCAM-armed beads, while treatment with 5 mM EDTA, which sequesters divalent cations such as Mn^{++}, abrogated the ability of MAdCAM-1 to capture virions; in both conditions, there was no significant change in virion-capture activity by mAb ACT-1, whose binding is insensitive to cation concentrations. Also, as expected, treatment with the inhibitory peptide ELN at 50 nM specifically abrogated MAdCAM-mediated virion capture, but had no effect on ACT-1-mediated capture (Fig. 3).

Virion-incorporated α4β7 promotes capture by and infection of MAdCAM-expressing cells

Having demonstrated that all HIV-1 progenies produced in activated human PBMC incorporate to some extent α4β7, even when grown in the absence of RA treatment, we engineered ‘all-or-nothing’ HIV-1 progenies both for a full-length infectious HIV-1 molecular clone, THRO.18 (fig. S5), as well as for pseudoviruses bearing the HIV-1 BaL envelope (fig. S6) (35). These homologous $\alpha4\beta7^{+}$ and $\alpha4\beta7^{-}$ viruses provided essential tools to investigate the impact of α4β7 incorporation on HIV-1 capture, infectivity and tissue homing. To obtain proof-of-concept of α4β7-mediated virion capture and transfer to susceptible target cells, we initially used an experimental model based on plate-immobilized MAdCAM-1. Plastic plates were coated with either soluble MAdCAM-1, or an irrelevant adhesion molecule, PECAM, and incubated with either $\alpha4\beta7^{+}$ or $\alpha4\beta7^{-}$ infectious viral progenies to allow for virion capture; then, unbound virus was extensively washed off, and the wells were overlaid with susceptible target cells (TZM-bl). Robust infection was detected in MAdCAM-coated wells, but neither in PECAM-coated wells with $\alpha4\beta7^{+}$ virus, nor in PECAM- or MAdCAM-coated wells with $\alpha4\beta7^{-}$ virus (Fig. 4A).

To validate the above findings in a more physiologically-relevant model system, we transfected MAdCAM-1 into MAdCAM-negative cells and tested their ability to mediate *trans*-infection of susceptible target cells with either $\alpha4\beta7^{+}$ or $\alpha4\beta7^{-}$ virions. To minimize background HIV-1 binding to the cellular membrane, we utilized for these experiments a proteoglycan-deficient variant of the CHO cell line, CHOpgsA745 (36). After MAdCAM-1 transfection, the cells were incubated with either $\alpha4\beta7^{+}$ or $\alpha4\beta7^{-}$ virions, extensively washed, and then overlaid with susceptible target cells (TZM-bl). Infection was detected only when cells expressing MAdCAM-1 were incubated with $\alpha4\beta7^{+}$ virus, while all the other conditions did not yield detectable virus transfer to susceptible target cells (Fig. 4B). These data demonstrated that $\alpha4\beta7^{+}$ virions are efficiently captured by MAdCAM-

expressing cells, which in turn mediate *trans*-infection of bystander target cells, illustrating a potential model of MAdCAM-mediated capture of $\alpha4\beta7^+$ HIV-1 virions by endothelial cells in intestinal HEV, with subsequent delivery to $CD4^+$ T cells extravasating into the gut mucosa.

To investigate whether the presence of α4β7 on the HIV-1 virion surface may directly promote infection of susceptible MAdCAM-expressing target cells, such as a unique subset of DC in mesenteric lymph nodes that were recently shown to express MAdCAM-1 in rhesus macaques (8), we transfected TZM-bl cells with MAdCAM-1 and tested their susceptibility to infection by $\alpha4\beta7^+$ and $\alpha4\beta7^-$ HIV-1 BaL pseudoviruses. As expected, infection was detected in both MAdCAM-1^+ and MAdCAM-1^- TZM-bl cells; however, the infection levels were significantly higher in MAdCAM-expressing cells infected with $\alpha4\beta7^+$ pseudoviruses compared to the same cells infected with $\alpha4\beta7^-$ pseudoviruses, whereas no difference was seen between the two pseudovirus progenies in MAdCAM-negative cells (Fig. 4C). These results suggest that α4β7 incorporation may facilitate infection of MAdCAM-expressing susceptible target cells.

Functional α4β7 is present in circulating virions from HIV-infected patients and SIV-infected macaques

To evaluate the physiological relevance of α4β7 incorporation into HIV-1 virions, we investigated whether and to what extent this phenomenon occurs *in vivo* in HIV-infected patients. For this purpose, we tested incorporation of functional α4β7 into circulating virus in a panel of sera obtained from viremic HIV-infected patients (37) using MAdCAM-1-armed magnetic beads in the virion-capture assay; as a control, we used beads armed with ICAM-1, the ligand of integrin LFA-1. Virion incorporation of α4β7 was detected in all the patient sera tested, with significantly higher levels in sera from patients during the early stages of HIV-1 infection compared with patients with chronic infection; in contrast, incorporation of LFA-1 was consistently lower in both patient groups (Fig. 5). These results indicated that virus circulating *in vivo* in HIV-infected patients consistently incorporates functional α4β7, corroborating the physiological relevance of this phenomenon. The higher levels of α4β7 incorporation detected during the early stages of HIV-1 infection are consistent with the extensive viral replication in $\alpha4\beta7^{hi}$ intestinal $CD4^+$ T cells during this critical phase of infection (1–4, 38).

As we demonstrated that SIV virions can incorporate α4β7 as efficiently as HIV-1 virions, and due to the logistic difficulties in obtaining sequential samples from acutely HIV-1-infected patients, we analyzed longitudinal plasma samples obtained from rhesus macaques experimentally infected with SIVmac239 throughout the course of acute primary infection (39). Although all the macaque plasma samples tested contained virion-incorporated α4β7, longitudinal analysis showed that α4β7 incorporation was highest during acute SIV infection (< 14 weeks of infection) and then progressively declined during the post-acute phase (> 14 weeks; Fig. 6A). A significant difference was observed by comparison of samples obtained before and after the first 14 weeks of infection (Fig. 6B). These data confirmed that the efficiency of α4β7 incorporation in circulating virions correlates with the

relative prevalence of α4β7 ^{hi} CD4$^+$ T cells in the gut compartment, which are progressively depleted following the acute phase of infection (1–4, 31, 38, 40, 41).

Virion-incorporated α4β7 promotes *in vivo* HIV-1 uptake by intestinal Peyer's patches

Since virion-incorporated α4β7 functionally interacts with its cognate ligand, MAdCAM-1, we postulated that virions bearing α4β7 within their envelope might specifically home into the intestinal compartment *in vivo*, where MAdCAM-1 is expressed at high levels (7). To test this hypothesis, we performed *in vivo* virion-homing experiments in a mouse model, as murine MAdCAM-1 efficiently binds to human α4β7 (42). Thus, we produced fluorescent HIV-1 virions, NL4.3-Gag EGFP (43), engineered to express α4β7, and we injected them into the tail vein of C57BL/6 mice, while homologous α4β7-negative (α4β7$^-$) virions were injected into control mice. Fluorescent HIV-1 virions with incorporated α4β7 were efficiently captured along the lumen of HEV in Peyer's patches at 45 minutes post-injection, whereas mice injected with α4β7$^-$ virus did not show any detectable virus homing to the gut tissue; homing of α4β7$^+$ virus into Peyer's patches was specifically blocked by the anti-α4β7 mAb ACT-1, whereas an isotype-control antibody had no effect (Fig. 7A, top row). Figure 7B shows three-dimensional reconstructions of the images in Fig. 7A, top row, which precisely illustrate the localization of α4β7$^+$ virions captured by HEV within Peyer's patches (see also animation in movie S1). Quantification of virus particles in three-dimensional image reconstructions demonstrated a significant reduction in virus homing to the Peyer's patches when the virus was blocked with mAb ACT-1 (Fig. 7C). Examination of control tissues showed that the spleen contained equivalent amounts of captured α4β7$^+$ and α4β7$^-$ virions (Fig. 7A, bottom row), while no significant uptake of either virus was seen in inguinal lymph nodes (Fig. 7A, middle row). Taken together, these data provide evidence for the selective and specific homing of α4β7$^+$ HIV-1 virions into the gut, suggesting that α4β7 incorporation may be a virulence factor that promotes and sustains HIV-1 infection of the intestinal compartment.

DISCUSSION

The present study describes how HIV-1 exploits a eukaryotic mechanism of cellular homing as a virulence factor to facilitate its own spread and pathogenesis. In support of the physiological role of virion-incorporated α4β7, we found that the integrin displayed on the surface of HIV-1 virions is functionally active, in that it binds specifically to its cognate ligand, MAdCAM-1. Consistent with previous data obtained for ICAM-1 and HLA-DR incorporation, we found that the core protein of HIV-1, Gag, is the main viral component involved in α4β7 capture/enrichment (30, 44, 45). The functional competence of virion-incorporated α4β7 was further validated by our *in vivo* homing experiments, which documented a selective and specific uptake of α4β7$^+$ but not α4β7-HIV-1 particles by Peyer's patches in the gut tissue of mice. The physiological relevance of virion-incorporated α4β7 was corroborated by its consistent presence in circulating virions from both HIV-infected patients and SIV-infected macaques. In particular, the detection of higher levels of virion-incorporated α4β7 during the early stages of infection, compared with the chronic stages, supports the biological significance of this phenomenon, as the pool of HIV-1 target cells that can efficiently produce α4β7$^+$ virions is drastically reduced upon depletion of

intestinal α4β7^{hi} CD4^{+} T cells following the acute phase of infection. Thus, the ability of virion-incorporated α4β7 to induce mucosal homing/retention of HIV-1 *in vivo* can have a major impact on viral transmission and pathogenesis, especially during the early stages of infection when the gut mucosa is still populated with CD4^{+} T cells expressing high levels of α4β7 (1–4, 31, 38, 40, 41).

Incorporation of α4β7 into HIV-1 virions may provide an additional and complementary mechanism to explain the protective effects observed upon infusion of a primatized anti-α4β7 antibody (ACT-1) in a series of seminal studies performed in SIV-challenged macaques (11–13). Our data suggest that, besides its effects on CD4^{+} T-cell trafficking and infection at mucosal sites, the anti-α4β7 antibody administered to macaques prior to (12) or early in the course (11) of acute primary infection may directly engage the integrin present on the virion surface, thereby interrupting key events in virus transmission and mucosal colonization. Of note, antibody localization data showed that the infused anti-α4β7 mAb efficiently reached all the anatomical sites examined (11, 12) and thus it could directly bind to virion-incorporated α4β7 in different body compartments. More challenging is the interpretation of the recent results obtained in macaques receiving anti-α4β7 antibody early in the course of chronic infection (46). In those animals, prolonged suppression of viral rebound for as long as two years was observed following discontinuation of both ART and anti-α4β7 antibody, but the underlying mechanism remains unclear (13). It has been hypothesized that perhaps the regimen of ART plus anti-α4β7 antibody induced an unusually effective immune response in the animals that ultimately controlled viral rebound, which would explain the persistence of the effect after antibody washout. Our results show that HIV-1 virions can be directly targeted by the anti-α4β7 antibody, indicating another possible mechanism to explain the prolonged suppression of viral rebound in macaques (13). In this regard, we hypothesize that the anti-α4β7 antibody might act via opsonization of circulating α4β7^{+} virus, promoting not only its rapid clearance via Fc-receptor-mediated mechanisms but also its efficient uptake and processing by antigen-presenting cells, leading to the induction of quantitatively and qualitatively more effective humoral and cell-mediated immune responses. Pre-clinical studies in nonhuman primates need to be carried out to test this hypothesis. Furthermore, important insights on the mechanisms of long-term virus control may come from the study of protection correlates in a recently initiated clinical trial with Vedolizumab, a clinically approved humanized form of the ACT-1 antibody (47–50), in HIV-infected individuals undergoing ART interruption (see ClinicalTrials.gov, Identifier: NCT02788175).

Although the present study establishes that functional α4β7 is incorporated into HIV-1 and SIV virions both *in vitro* and *in vivo*, and promotes intestinal homing of HIV-1 virions *in vivo* in a murine model, it does not definitively prove whether these findings are relevant to the pathogenesis of HIV-1 or SIV infection. Further studies in macaques will be important to evaluate whether the presence of incorporated α4β7 can effectively enhance the transmission, spread and pathogenesis of SIV in a relevant *in vivo* model. Another limitation of our work is that it does not identify the precise molecular mechanism for the selective enrichment of α4β7 into nascent HIV-1 virions. Further studies are needed to define whether specific domains of HIV-1 Gag and α4 or β7 may directly interact to promote incorporation of α4β7 into maturing virions.

In conclusion, our results extend the paradigm of tissue homing to a subcellular organism and add another potential mechanism of pathogenesis to the rich armamentarium of virulence factors displayed by HIV-1. Although virion incorporation has been reported for several cellular proteins, the case of α4β7 may be particularly relevant to HIV-1 pathogenesis because of the central role played by this gut-homing integrin, and the gut compartment in general, in the physiology of HIV-1 infection. In addition, the presence of α4β7 on HIV-1 virions may also represent a facilitating factor for HIV-1 transmission via the mucosal route. This hypothesis, which is consistent with the reduced SIV transmission documented in macaques treated with anti-α4β7 antibody (12), awaits validation in future pre-clinical and clinical studies.

Materials and Methods

Study design

This study was designed to characterize the incorporation of integrin α4β7 into HIV-1 virions, to validate the *in vivo* relevance of this phenomenon in infected humans and monkeys, and to determine the effect of virion-incorporated a4β7 on virus trafficking *in vivo* in a mouse model. Experiments to characterize a4β7 incorporation into virion envelopes were performed on a wide range of HIV-1 isolates of different coreceptor usage phenotypes and genetic subtypes (n = 12). To determine the *in vivo* relevance of a4β7 incorporation, circulating virus was characterized in an unselected cohort of HIV-1 infected patients divided according to their stage of infection into acute (infected < 6 months, n = 19) and chronic (infected > 6 months, n = 14). Experimentally SIV-infected macaques (n = 11) were used for longitudinal analysis of a4β7 incorporation from early acute infection (week 2 post-infection) through to chronic disease (week 40 post-infection).

Antibodies and recombinant proteins

The mAbs utilized for cell surface staining and virion incorporation studies included the following: anti-CD49d [α4], anti-integrin β7, anti-CD29 [β1], anti-CD54 [ICAM-1], anti-CD11a [LFA-1], anti-HLA-ABC, anti-HLA-DR, anti-CD27, anti-CD43 [leukosialin], anti-CD45 [protein tyrosine phosphatase, receptor type, C], anti-CD46 [membrane cofactor protein] (BD Biosciences); anti-CD102 [ICAM-2], anti-CD4 [OKT-4], anti-Mouse IgG (eBioscience); anti-MAdCAM-1 (clone 314G8, BioRad); and mouse IgG1 (R&D Systems). Mouse and primatized forms of the anti-α4β7 monoclonal antibody ACT-1 and corresponding isotype control IgG1 were obtained from Dr. A. A. Ansari (mouse ACT-1 through the NIH AIDS Reagent Program, NIAID, NIH). Recombinant proteins included: human Fc-chimeric MAdCAM-1, human Fc-chimeric ICAM-1, and human α4β7 (all 3 from R&D Systems), and human Fc-chimeric PECAM (ACRO Biosystems).

Flow cytometry

Cells were stained with mAbs for 1 hr at 4°C, washed with PBS and incubated for 30 minutes at 4°C with PE-conjugated sheep anti-mouse IgG (Sigma). All mAbs were previously titrated with 8-point dilution curves by flow cytometry on activated human PBMC, and used for both cell-surface staining and virion capture (see below) at the highest concentration yielding less than 90% binding. Flow cytometry was performed using a BD

FACS Canto (Becton Dickinson) and analyzed with FlowJo software version 9.5.2 for Macintosh (TreeStar).

Virion-capture assays

Protein G-conjugated immunomagnetic beads (Dynabeads; Life Technologies) were armed with the appropriate antibody or recombinant protein for 20 min at room temperature (30 μL/reaction) and then washed three times with PBS containing 0.025% (wt/vol) casein to extensively remove the unbound antibody or protein. All antibodies were titrated with 8-point dilution curves by flow cytometry, and used for both cell-surface staining and virion capture at the highest concentration yielding less than 90% binding. For laboratory-grown HIV-1 and SIV viruses, data were normalized based on the input $p24_{Gag}$ or $p27_{Gag}$ protein concentrations used (10–20 ng/reaction). Recombinant proteins (human Fc-chimeric MAdCAM-1 or ICAM-1) were used at 1 μg/ml. For functional tests, the virus stocks were pre-incubated for 15 min with or without α4β7 activators (1 mM $MnCl_2$) or inhibitors (5 mM EDTA, 50 nM ELN-4757772) (34). For virion capture on patient or monkey sera/plasma, the assays were performed with MAdCAM-1-or ICAM-1-armed beads in the presence of 2 mM $MnCl_2$. The data were normalized based on the input volumes used for each patient or animal (200–380 μl/reaction). All virion-capture assays were performed by incubating washed immunomagnetic beads, pre-armed with antibodies or recombinant Fc-chimeric proteins, with $p24_{Gag}$-/$p27_{Gag}$-normalized amounts of HIV-1/SIV viral stocks or with equal volumes of serum/plasma for 2 hours at room temperature. Beads were then washed 3 times with PBS-casein to extensively remove unbound virus particles and either treated with 0.5% Triton X-100 to lyse the captured virions for p24 quantification, or directly incubated with viral lysis buffer from the QIAamp Viral RNA Mini Kit for viral RNA quantification by real-time PCR.

Viral isolates and infection assays

To generate virion progenies, PBMC were isolated from BuffyCoats obtained from healthy donors, activated with 5 μg/ml of phytohemagglutinin (PHA; Sigma, St. Louis, MO) or with 1 μg/ml of mAb OKT3 in complete RPMI medium (Invitrogen, Carlsbad, CA) containing 10% fetal bovine serum (FBS, Hyclone, Thermo Scientific, Waltham, MA), recombinant human IL-2 (Roche Applied Science, Mannheim, Germany), glutamine at 2 mM, streptomycin at 50 μg/mL, and penicillin at 100 U/mL for 72 hr prior to HIV-1 infection; when noted, 10nM retinoic acid (RA, Sigma) was also added at the time of initial stimulation. Primary HIV-1 isolates 92HT599, 97ZA009, 92UG037, 93UG065, 93TH057, CMU06 and 97BR019 were obtained from the NIH AIDS Reagent Program; the other isolates were obtained in our laboratory from the peripheral blood of HIV-infected patients followed at the NIAID AIDS Clinic. All the clinical isolates were minimally passaged (once or twice) in human PBMC *in vitro*. SIV isolates smE660.307 (51) and mac251.745 (39) were obtained in our laboratory from the peripheral blood of chronically infected in paientss and expanded in activated human PBMC.

p24 quantification by AlphaLISA

To quantify HIV-1 p24 in viral stocks and normalize virus inputs for *in vivo* assays and capture conditions, as well as to quantify the amount of captured HIV-1 virions, we used a

high-sensitivity AlphaLISA p24 detection kit on an EnSpire MultiMode Plate Reader (Perkin Elmer), according to the manufacturer's protocols.

Western blot analysis and quantification of incorporated proteins

Western blot was used for semi-quantitative evaluation of virion incorporation of α4β7 and gp120 (26). SDS-PAGE was performed on polyethylene glycol treatment (PEG)-concentrated HIV-1 SF162 viral lysates (75 ng of virion-associated p24 per well) produced by untreated PBMC (RA^-) versus RA-treated PBMC (RA^+). Western blot analysis of α4 expression was performed with anti-integrin α4/CD49d rabbit polyclonal antibody (Thermo Fisher) and reveled with anti-rabbit IgG-HRP (Sigma). The integrin α4 detected in the $CD4^+$ T-cell lysate (lane 1) and in progeny virion lysates (middle two lanes, RA^+ and RA^-) is the cleaved molecular form migrating at ~70kDa, which is the prevalent form expressed on the surface of activated T cells (31), whereas the recombinant α4 protein used as reference (lanes 2–4) migrated at 150kDa, which is the expected molecular weight of the uncleaved mature protein (52). Membranes were re-probed to confirm equal loading of SF162 lysates (HIV $p24_{Gag}$ input) by blotting with pooled HIV-1-infected patient sera and revealing withgoat anti-human IgG-HRP (Sigma). Blotting with anti-gp120 mAb (b24; a kind gift of George K. Lewis) and revealing with anti-mouse IgG-HRP (Sigma) was used to estimate the concentration of virion-incorporated gp120 envelope glycoprotein. Quantification of incorporated α4β7 and gp120 was performed by densitometric scanning (Image Studio Lite software) of the bands followed by interpolation of the results on the curves obtained with the recombinant proteins used as reference.

Molecular clones and transfection

The full-length infectious HIV-1 molecular clones THRO. 18 and NL4-3 were obtained through the NIH AIDS Reagent Program. Plasmids expressing human α4 and β7 integrin subunits were obtained from OriGene Technologies, Inc. To produce 'all-or-nothing' viral progenies with and without α4β7, 293T cells were transfected using TransIT-293 Transfection Reagent (Mirus Bio LLC). Briefly, 0.5×10^6 cells/well were plated into 6-well plates overnight. For each well, 1 μ*g* of subunits α4 and β7 together with 2 μg of each virus clone were diluted in Opti-MEM, followed by a 1:4 (DNA:reagent) dilution of TransIT-293 transfection reagent into the DNA-Opti-MEM mixture. After 30 min at room temperature, the transfection mixtures were added dropwise to the cells in complete DMEM. The medium was replaced 16 hours post-transfection, and virus was harvested 48 hours after medium replacement and frozen in aliquots to avoid repeated freeze-thaw cycles. CHOpgsA745 cells (a kind gift of Jeffrey Esko) were plated (0.8×10^6 per 6-well) the day before and then transfected with 4 μg of MAdCAM-1 plasmid using a similar protocol. Viral pseudoparticles expressing gp160 from HIV-1 BaL were produced in HEK 293T cells by co-transfecting gp160-expressing plasmid together with a backbone plasmid, $pSG3^{\Delta env}$, obtained from John C. Kappes and Xiaoyun Wu through the NIH AIDS Reagent Program, Division of AIDS, NIAID, NIH (53, 54). To assess the role of the Gag and Env viral components in virion incorporation of α4β7, 293T cells were transfected to express the codon-optimized 96ZM651.8 clone of full-length HIV-1 Gag (NIH AIDS Reagent Program) on its own, or co-expressed with HIV-1 Env (BaL gp160) in the presence or absence of plasmids expressing the α4 and β7 integrin subunits. Fluorescent HIV-1 NL4.3 Gag EGFP virus particles were

produced by transfecting 293T cells with the plasmid (a kind gift of Walther Mothes) with or without α4 and β7; viral progenies were harvested ~72 hr post-transfection. We assessed the levels of gp120 and Env trimer expression after α4 and β7 cotransfection using a panel of anti-Env mAbs by flow cytometry and found that the addition of α4 and β7 plasmids did not significantly affect the amount of HIV-1 Env expression (figs. S5 and S6).

HIV-1 and SIV quantification in infected patients and macaques by real-time PCR

HIV-1 and SIV RNA levels in patient and macaque plasma/serum, respectively, as well as in virion-capture assays were measured using quantitative real-time RT-PCR assays. Viral RNA was purified using the QIAamp Viral RNA kit (Qiagen, USA). The number of SIV RNA genome equivalents was determined using a single-tube real-time RT-RCR assay based on the AgPath-ID One-Step RT-PCR Kit (Applied Biosystems, USA), using previously reported primers, probe and amplification conditions (39). The number of HIV-1 genome equivalents was obtained in a similar manner using previously reported primers, probe and amplification conditions (55). Patients with acute and chronic HIV-1 infection were followed at the NIAID AIDS Clinic, Bethesda, Maryland, and the UNC Project Malawi, Lilongwe, Malawi. Archival plasma samples from rhesus macaques infected with SIVmac251 were from a previous study (39).

In vivo HIV-1 homing experiments

C57BL/6 mice, 8–12 weeks of age, were obtained from Jackson Laboratory and housed under specific-pathogen-free conditions. All the animal experiments and protocols used in the study were approved by the NIAID Animal Care and Use Committee (ACUC) at the NIH. Reverse-transcriptase-defective fluorescent HIV-1 NL4.3 Gag EGFP virus particles, either $\alpha4\beta7^{-}$ or $\alpha4\beta7^{+}$, were injected into the tail vein (50 ng of total $p24_{Gag}$ inoculum for each virus). For antibody-mediated blocking, the viral stocks were pre-incubated with 200 μg per inoculum of primatized anti-α4β7 mAb ACT-1 or with the corresponding primatized isotype-control antibody (IgG1) for 30 min at 4°C. The antibodies were the same used in previous *in vivo* studies in macaques (11, 12) and kindly provided by Dr. A. Ansari. After 45 minutes, the mice were euthanized and lymph nodes, Peyer's patches, and spleens were collected. The tissues were fixed in newly prepared 4% paraformaldehyde (Electron Microscopy Science) overnight at 4°C on an agitation stage, and then embedded in 4% low-melting agarose (Invitrogen) in PBS and sectioned with a vibratome (Leica VT-1000 S) at a 30 μm thickness. Thick sections were blocked in PBS containing 10% FBS, 1 mg/ml anti-Fcγ receptor antibody (BD Biosciences), and 0.1% Triton X-100 (Sigma) for 30 minutes at room temperature. Sections were stained overnight at 4°C on an agitation stage with the following antibodies: anti-CD4 (RM4-5, BD Biosciences), anti-CD169 (3D6.112, BioLegend), and anti-PNAd (BD PharmingenTM, clone: MECA-79). Stained thick sections were microscopically analyzed using a Leica SP5 confocal microscope (Leica Microsystem, Inc.) and images were processed with Leica LAS AF software (Leica Microsystem, Inc.) and Imaris software v.7.7.1 64x (Bitplane AG). Confocal microscopy was performed using a previously published protocol (56).

Statistical analyses

Differences in the efficiency of virion incorporation and cell-surface expression of lymphocyte markers (Figs. 1C, 1D and S3) were evaluated by paired 2-tailed t-test; differences in the extent of integrin incorporation into virions between patient and macaque groups (Figs. 5 and 6B) were evaluated by unpaired 2-tailed t-test. *In vivo* homing experiments were performed three times using two mice per experimental group, and the results shown in Fig. 7C represent mean values of at least triplicate samples from each tissue. Standard errors of the mean (SEM) and *p* values were calculated with ordinary one-way ANOVA. All statistical tests were performed using GraphPad Prism 6 (GraphPad software).

Supplementary Material

Refer to Web version on PubMed Central for supplementary material.

Acknowledgments

We thank Raffaello Cimbro, Hana Schmeisser, Aftab A. Ansari, and Siddappa N. Byrareddy for helpful discussion, Aftab A. Ansari for murine and primatized anti-α4β7 mAb ACT-1 and isotype control antibody (IgG1), Walther Mothes for the HIV-1 NL4.3 Gag EGFP plasmid, Jeffrey Esko for providing CHOpsgA475 cells (through ATCC), George K. Lewis for mAb b24, the AIDS Reagent Program for providing reagents, the volunteers and staff of the NIH Clinical Center Blood Bank, and the patients and nurses of the NIAID AIDS Clinic. The clinical protocols for obtaining patient serum and for experimental SIV infection in macaques were approved by the relevant NIH committees.

Funding:

This research was supported by the Intramural Program of the Vaccine Research Center and the Division of Intramural Research, NIAID, NIH, and by Grants from the Duke Center for HIV Vaccine Immunology and Immunogen Discovery, and from the NIH (R01 DK 108424) to M.C. This research was also made possible through the NIH Medical Research Scholars Program (MRSP), a public-private partnership supported jointly by the NIH and the Doris Duke Charitable Foundation, the Howard Hughes Medical Institute, the American Association for Dental Research, the Colgate-Palmolive Company, and other private donors through the Foundation for the NIH (for a complete list, see http://www.fnih.org).

References and Notes

1. Brenchley JM, Douek DC. HIV infection and the gastrointestinal immune system. Mucosal Immunol. 2008; 1:23–30. [PubMed: 19079157]
2. Li Q, et al. Peak SIV replication in resting memory CD4+ T cells depletes gut lamina propria CD4+ T cells. Nature. 2005; 434:1148–1152. [PubMed: 15793562]
3. Haase AT. Perils at mucosal front lines for HIV and SIV and their hosts. Nat Rev Immunol. 2005; 5:783–792. [PubMed: 16200081]
4. Brenchley JM, et al. CD4+ T cell depletion during all stages of HIV disease occurs predominantly in the gastrointestinal tract. J Exp Med. 2004; 200:749–759. [PubMed: 15365096]
5. Arthos J, et al. HIV-1 envelope protein binds to and signals through integrin alpha4beta7, the gut mucosal homing receptor for peripheral T cells. Nat Immunol. 2008; 9:301–309. [PubMed: 18264102]
6. Cicala C, Arthos J, Fauci AS. HIV-1, envelope integrins and co-receptor use in mucosal transmission of HIV. J Transl Med. 2011; 9(Suppl 1):S2. [PubMed: 21284901]
7. Briskin M, et al. Human mucosal addressin cell adhesion molecule-1 is preferentially expressed in intestinal tract and associated lymphoid tissue. Am J Pathol. 1997; 151:97–110. [PubMed: 9212736]
8. Guerra-Perez N, et al. Retinoic acid imprints a mucosal-like phenotype on dendritic cells with an increased ability to fuel HIV-1 infection. J Immunol. 2015; 194:2415–2423. [PubMed: 25624458]

9. Iwata M, et al. Retinoic acid imprints gut-homing specificity on T cells. Immunity. 2004; 21:527–538. [PubMed: 15485630]
10. Lampen A, Meyer S, Arnhold T, Nau H. Metabolism of vitamin A and its active metabolite all-trans-retinoic acid in small intestinal enterocytes. J Pharmacol Exp Ther. 2000; 295:979–985. [PubMed: 11082432]
11. Ansari AA, et al. Blocking of alpha4beta7 gut-homing integrin during acute infection leads to decreased plasma and gastrointestinal tissue viral loads in simian immunodeficiency virus-infected rhesus macaques. J Immunol. 2011; 186:1044–1059. [PubMed: 21149598]
12. Byrareddy SN, et al. Targeting alpha4beta7 integrin reduces mucosal transmission of simian immunodeficiency virus and protects gut-associated lymphoid tissue from infection. Nat Med. 2014; 20:1397–1400. [PubMed: 25419708]
13. Byrareddy SN, et al. Sustained virologic control in SIV+ macaques after antiretroviral and alpha4beta7 antibody therapy. Science. 2016; 354:197–202. [PubMed: 27738167]
14. Fraser C, et al. Virulence and pathogenesis of HIV-1 infection: an evolutionary perspective. Science. 2014; 343:1243727. [PubMed: 24653038]
15. Arthur LO, et al. Cellular proteins bound to immunodeficiency viruses: implications for pathogenesis and vaccines. Science. 1992; 258:1935–1938. [PubMed: 1470916]
16. Martin G, Tremblay MJ. HLA-DR, ICAM-1, CD40, CD40L, and CD86 are incorporated to a similar degree into clinical human immunodeficiency virus type 1 variants expanded in natural reservoirs such as peripheral blood mononuclear cells and human lymphoid tissue cultured ex vivo. Clin Immunol. 2004; 111:275–285. [PubMed: 15183148]
17. Tremblay MJ, Fortin JF, Cantin R. The acquisition of host-encoded proteins by nascent HIV-1. Immunol Today. 1998; 19:346–351. [PubMed: 9709501]
18. Bounou S, Leclerc JE, Tremblay MJ. Presence of host ICAM-1 in laboratory and clinical strains of human immunodeficiency virus type 1 increases virus infectivity and CD4(+)-T-cell depletion in human lymphoid tissue a major site of replication in vivo. J Virol. 2002; 76:1004–1014. [PubMed: 11773376]
19. Fortin JF, Cantin R, Lamontagne G, Tremblay M. Host-derived ICAM-1 glycoproteins incorporated on human immunodeficiency virus type 1 are biologically active and enhance viral infectivity. J Virol. 1997; 71:3588–3596. [PubMed: 9094631]
20. Rizzuto CD, Sodroski JG. Contribution of virion ICAM-1 to human immunodeficiency virus infectivity and sensitivity to neutralization. J Virol. 1997; 71:4847–4851. [PubMed: 9151884]
21. Tardif MR, Tremblay MJ. Presence of host ICAM-1 in human immunodeficiency virus type 1 virions increases productive infection of CD4+ T lymphocytes by favoring cytosolic delivery of viral material. J Virol. 2003; 77:12299–12309. [PubMed: 14581566]
22. Auerbach DJ, et al. Identification of the platelet-derived chemokine CXCL4/PF-4 as a broad-spectrum HIV-1 inhibitor. Proc Natl Acad Sci U S A. 2012; 109:9569–9574. [PubMed: 22645343]
23. Cimbro R, et al. Tyrosine sulfation in the second variable loop (V2) of HIV-1 gp120 stabilizes V2-V3 interaction and modulates neutralization sensitivity. Proc Natl Acad Sci U S A. 2014; 111:3152–3157. [PubMed: 24569807]
24. Cimbro R, et al. Tyrosine-sulfated V2 peptides inhibit HIV-1 infection via coreceptor mimicry. EBioMed. 2016; 10:45–54.
25. The virion capture-assay was performed according to the previously reported method (22–24) with further validation for the specific HIV-1 strain used (fig. S1). Immunomagnetic beads armed with mAbs against cell-surface markers were tested on a defined viral stock of the CCR5-tropic (R5) HIV-1 isolate BaL produced in primary human peripheral blood mononuclear cells (PBMC) activated with anti-CD3 mAb (OKT3) with or without the addition of RA to induce high levels of $\alpha 4\beta 7$ expression. In parallel, the same panel of mAbs was used in flow cytometry to evaluate surface expression of the same markers on the homologous HIV-producer cells. To normalize the amount of antibody to be used in parallel capture/staining experiments, all the mAbs were initially titrated by flow cytometry, and the highest concentration below that yielding ≥90% binding was selected. Thus, even though the absolute binding efficiency of the different mAbs could not be directly compared, the relative efficiency of cell-surface binding vs. HIV-1 virion capture was normalized.

26. Esser MT, et al. Differential incorporation of CD45, CD80 (B7-1), CD86 (B7-2), and major histocompatibility complex class I and II molecules into human immunodeficiency virus type 1 virions and microvesicles: implications for viral pathogenesis and immune regulation. J Virol. 2001; 75:6173–6182. [PubMed: 11390619]
27. Meerloo T, et al. Host cell membrane proteins on human immunodeficiency virus type 1 after in vitro infection of H9 cells and blood mononuclear cells. An immuno-electron microscopic study. J Gen Virol. 1993; 74(Pt 1):129–135. [PubMed: 8093711]
28. Nguyen DH, Hildreth JE. Evidence for budding of human immunodeficiency virus type 1 selectively from glycolipid-enriched membrane lipid rafts. J Virol. 2000; 74:3264–3272. [PubMed: 10708443]
29. Lazarovits AI, et al. Lymphocyte activation antigens. I. A monoclonal antibody, anti-Act I, defines a new late lymphocyte activation antigen. J Immunol. 1984; 133:1857–1862. [PubMed: 6088627]
30. Jalaguier P, Cantin R R, Maaroufi H, Tremblay MJ. Selective acquisition of host-derived ICAM-1 by HIV-1 is a matrix-dependent process. J Virol. 2015; 89:323–36. [PubMed: 25320314]
31. Kelly KA, Rank RG. Identification of homing receptors that mediate the recruitment of CD4 T cells to the genital tract following intravaginal infection with Chlamydia trachomatis. Infect Immun. 1997; 65:5198–5208. [PubMed: 9393816]
32. Tiwari S, Askari JA, Humphries MJ, Bulleid NJ. Divalent cations regulate the folding and activation status of integrins during their intracellular trafficking. J Cell Sci. 2011; 124:1672–1680. [PubMed: 21511727]
33. Zhang K, Chen J. The regulation of integrin function by divalent cations. Cell Adh Migr. 2012; 6:20–29. [PubMed: 22647937]
34. Xu YZ, et al. Orally available and efficacious alpha4beta1/alpha4beta7 integrin inhibitors. Bioorg Med Chem Lett. 2013; 23:4370–4373. [PubMed: 23777782]
35. Homologous α4β7+ and α4β7^{-} viral progenies were obtained by co-transfecting 293T cells, which do not constitutively express α4β7, with a full-length infectious HIV-1 clone, THR0.18, with or without plasmids expressing the α4 and β7 integrin subunits. The resulting viral progenies were confirmed to be either positive or completely negative for α4β7 incorporation (Fig. S5). Likewise, we engineered α4β7+ and α4β7^{-} infectious HIV-1 pseudoparticles by co-transfecting an HIV-1 envelope-deficient backbone with a plasmid expressing full-length HIV-1 BaL gp160, with or without plasmids expressing the α4 and β7 subunits (Fig. S6).
36. Esko JD, Stewart TE, Taylor WH. Animal cell mutants defective in glycosaminoglycan biosynthesis. Proc Natl Acad Sci U S A. 1985; 82:3197–3201. [PubMed: 3858816]
37. Patients were derived from two cohorts, one at the NIAID AIDS Clinic in Bethesda, MD, and one at the UNC Project Malawi in Lilongwe, Malawi. Patients were selected among those who had adequate samples stored in archive with significant levels of viremia (>50,000 HIV-1 RNA copies/mL) and included similar numbers of subjects with early infection (6 months or less from putative HIV-1 acquisition) and chronic infection (more than 6 months after HIV-1 acquisition).
38. Wang X, et al. Monitoring alpha4beta7 integrin expression on circulating CD4+ T cells as a surrogate marker for tracking intestinal CD4+ T-cell loss in SIV infection. Mucosal Immunol. 2009; 2:518–526. [PubMed: 19710637]
39. Vassena L, et al. Treatment with IL-7 prevents the decline of circulating CD4+ T cells during the acute phase of SIV infection in rhesus macaques. PLoS Pathog. 2012; 8:e1002636. [PubMed: 22511868]
40. Hawkins RA, Rank RG, Kelly KA. Expression of mucosal homing receptor alpha4beta7 is associated with enhanced migration to the Chlamydia-infected murine genital mucosa in vivo. Infect Immun. 2000; 68:5587–5594. [PubMed: 10992458]
41. McKinnon LR, et al. Characterization of a human cervical CD4+ T cell subset coexpressing multiple markers of HIV susceptibility. J Immunol. 2011; 187:6032–6042. [PubMed: 22048765]
42. Shyjan AM, Bertagnolli M, Kenney CJ, Briskin MJ. Human mucosal addressin cell adhesion molecule-1 (MAdCAM-1) demonstrates structural functional similarities to the alpha 4 beta 7-integrin binding domains of murine MAdCAM-1, but extreme divergence of mucin-like sequences. J Immunol. 1996; 156:2851–2857. [PubMed: 8609404]

43. Sewald X, et al. Retroviruses use CD169-mediated trans-infection of permissive lymphocytes to establish infection. Science. 2015; 350:563–567. [PubMed: 26429886]
44. Beausejour Y, Tremblay MJ. Envelope glycoproteins are not required for insertion of host ICAM-1 into human immunodeficiency virus type 1 and ICAM-1-bearing viruses are still infectious despite a suboptimal level of trimeric envelope proteins. Virology. 2004; 324:165–172. [PubMed: 15183063]
45. Martin G, Beausejour Y, Thibodeau J, Tremblay MJ. Envelope glycoproteins are dispensable for insertion of host HLA-DR molecules within nascent human immunodeficiency virus type 1 particles. Virology. 2005; 335:286–290. [PubMed: 15840527]
46. Cohen J. Surprising treatment 'cures' monkey HIV infection. Science. 2016; 354:157. [PubMed: 27738148]
47. Rosario M, et al. Vedolizumab pharmacokinetics pharmacodynamics, safety, and tolerability following administration of a single, ascending intravenous dose to healthy volunteers. Clin Drug Investig. 2016; 36:913–923.
48. Amiot A, et al. Effectiveness and Safety of Vedolizumab Induction Therapy for Patients With Inflammatory Bowel Disease. Clin Gastroenterol Hepatol. 2016
49. Jovani M, Danese S. Vedolizumab for the treatment of IBD: a selective therapeutic approach targeting pathogenic a4b7 cells. Curr Drug Targets. 2013; 14:1433–1443. [PubMed: 23980911]
50. Khanna R, Mosli MH, Feagan BG. Anti-Integrins in Ulcerative Colitis and Crohn's Disease: What Is Their Place? Dig Dis. 2016; 34:153–159. [PubMed: 26982012]
51. Lusso P, et al. Human herpesvirus 6A accelerates AIDS progression in macaques. Proc Natl Acad Sci U S A. 2007; 104:5067–5072. [PubMed: 17360322]
52. Pujades C, Teixido J, Bazzoni G, Hemler ME. Integrin alpha 4 cysteines 278 and 717 modulate VLA-4 ligand binding and also contribute to alpha 4/180 formation. Biochem J. 1996; 313(Pt 3): 899–908. [PubMed: 8611173]
53. Wei X, et al. Emergence of resistant human immunodeficiency virus type 1 in patients receiving fusion inhibitor (T-20) monotherapy. Antimicrob Agents Chemother. 2002; 46:1896–1905. [PubMed: 12019106]
54. Wei X, et al. Antibody neutralization and escape by HIV-1. Nature. 2003; 422:307–312. [PubMed: 12646921]
55. Malnati MS, et al. A universal real-time PCR assay for the quantification of group-M HIV-1 proviral load. Nat Protoc. 2008; 3:1240–1248. [PubMed: 18600229]
56. Park C, Arthos J, Cicala C, Kehrl JH. The HIV-1 envelope protein gp120 is captured and displayed for B cell recognition by SIGN-R1(+) lymph node macrophages. Elife. 2015; 4

HIV

Editorial Summary

Taking HIV to the gut

Antiretroviral therapy (ART) effectively limits HIV replication, but HIV+ individuals are medicated for life since ART withdrawal results in rebound of persistent virus. Developing therapies that keep viral loads low in the long-term and prevent reinfection remains an important goal – one emerging approach is an antibody against integrin α4β7. Integrin α4β7 is a receptor that facilitates homing of CD4+ T cells to the gut, a key site for HIV persistence. ART-suppressed macaques that received antibodies against integrin α4β7 controlled the virus even after ART withdrawal. Here, Guzzo *et al.* demonstrate that integrin α4β7 is incorporated into the HIV envelope suggesting that antibody treatment may directly interfere with the ability of HIV to target intestinal tissues. Their results change our perception of the role of integrin α4β7, a promising therapeutic target in HIV pathogenesis.

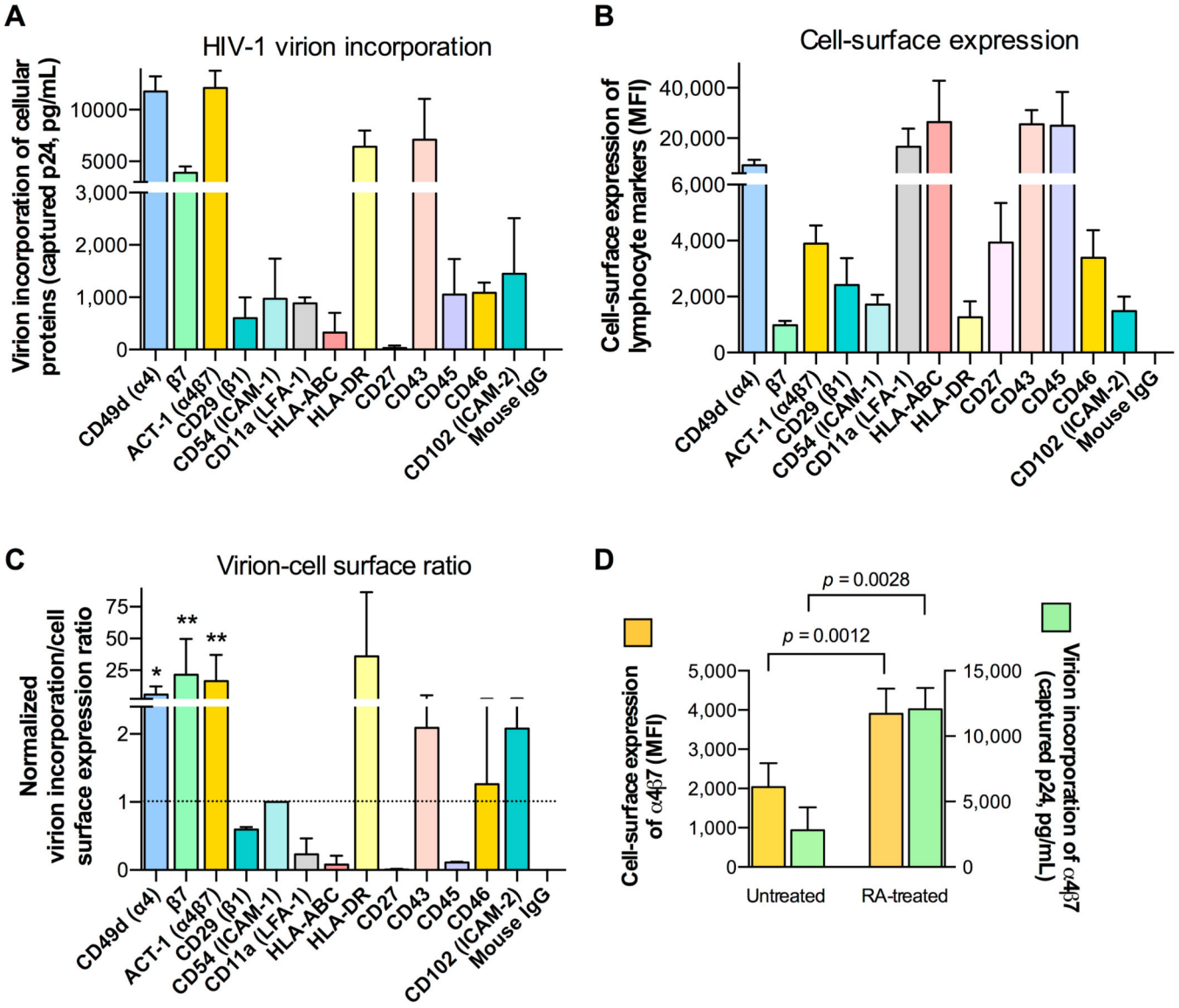

Fig. 1. HIV-1 virions efficiently incorporate integrin α4β7

(**A**) Immunomagnetic capture of virion progeny (HIV-1 SF162) produced by RA-activated human PBMC cells using mAbs directed against a panel of cell surface-expressed lymphocyte antigens. Captured virions from identical viral inputs were quantified for $p24_{Gag}$ antigen concentrations by AlphaLisa. The data represent the mean (±SD) of three biological replicates performed using PBMC from three different healthy blood donors. (**B**) Cell-surface staining of HIV-infected RA-activated human PBMC using the same panel of mAbs as in panel **A**. Mean fluorescence intensity (MFI) values obtained with normalized antibody concentrations are shown. The data represent the mean (±SD) of three biological replicates performed using virus produced by PBMC from three different healthy blood donors. (**C**) Ratio between virion incorporation and cell-surface expression for each lymphocyte marker, with the calculated ratio for ICAM-1 set at 1, as a reference. To obtain an index of incorporation efficiency, we first normalized the levels of both virion incorporation and cell-surface expression to the respective levels detected with ICAM-1, selected as a reference

protein; then, for each protein we calculated the ratio between normalized virion incorporation and normalized cell-surface expression. The incorporation of integrin α4β7 (mAb ACT-1) was significantly higher than that of ICAM-1. * $p = 0.025$; ** $p < 0.01$ by paired two-tailed t-test. (**D**) Parallel analysis of α4β7 cell-surface expression (yellow bars, left y-axis) and virion incorporation (green bars, right y-axis) in cultures of RA-treated and untreated human PBMC infected with HIV-1 SF162. The data represent the mean (±SD) of three biological replicates performed using PBMC and respective progeny virus from three different healthy blood donors.

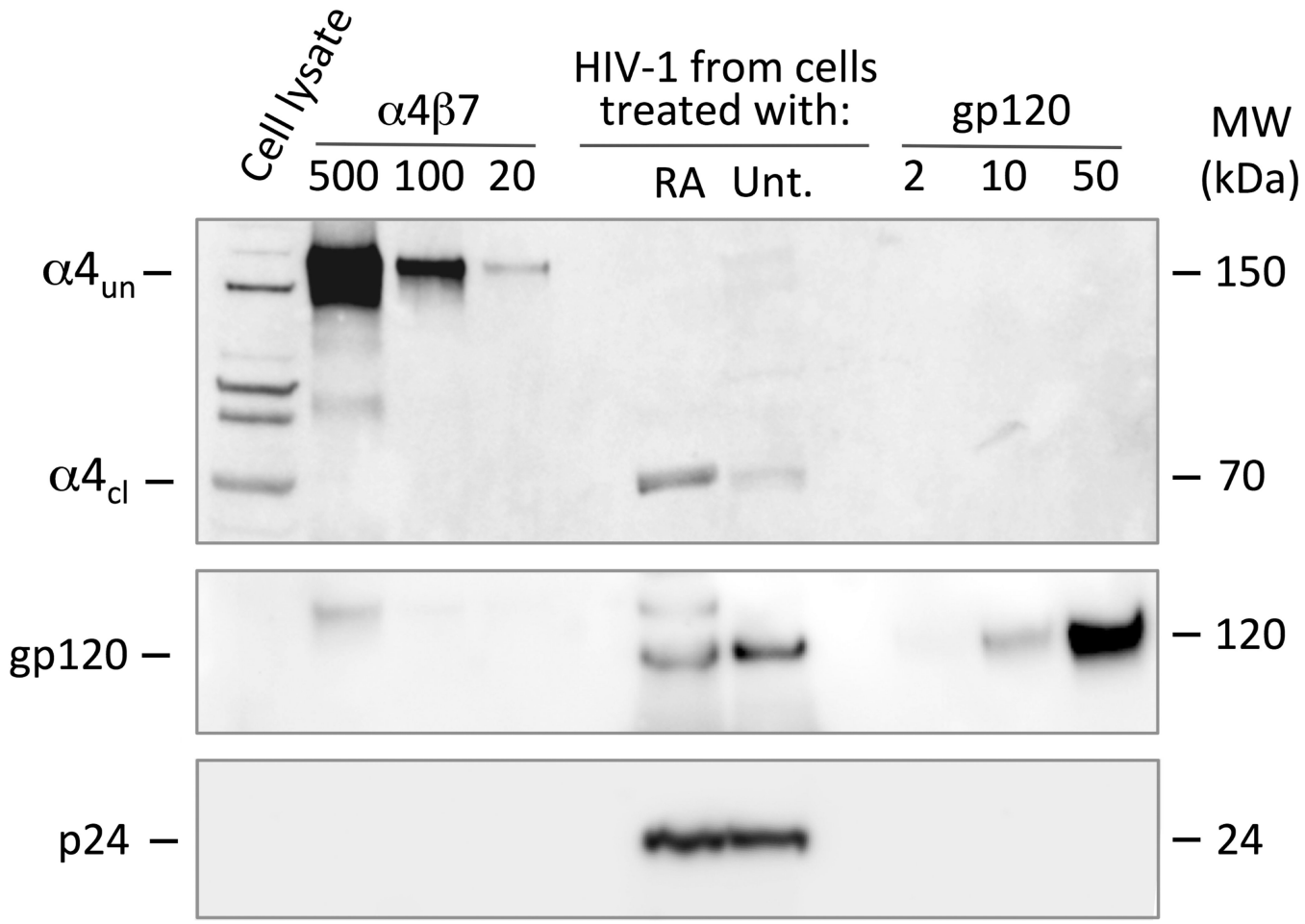

Fig. 2. Quantitative analysis of α4β7 incorporation by HIV-1 virions

Western blot analysis of α4 and HIV-1 structural proteins ($gp120_{Env}$ and $p24_{Gag}$) incorporated into HIV-1 virions produced by RA-treated human PBMC (RA) vs. untreated human PBMC (Unt.). Virus stocks were concentrated by PEG treatment and centrifugation before detergent lysis. As a control for integrin subunit expression on producer cells, we loaded whole cell lysate from RA-treated $CD4^+$ T cells. For semi-quantitative assessment of virion incorporation, we used serial dilutions of recombinant α4β7 and recombinant gp120, respectively, at the indicated amounts loaded per lane (in nanograms). The different molecular weight of recombinant α4 (120 kDa) vs. cell-derived α4 (70kDa) reflect the fact that activated T cells express cleaved α4 ($α4_{cl}$) on their surface, while recombinant α4 is uncleaved ($α4_{un}$). Semi-quantification of incorporated α4β7 and gp120 was performed by densitometric scanning and interpolation of the results on the curves obtained for the recombinant proteins used as reference. The gel was also developed using pooled sera from HIV-infected individuals (bottom panel) to verify the correct amount of input $p24G_ag$ antigen. This Western blot is representative of two experiments performed with similar results.

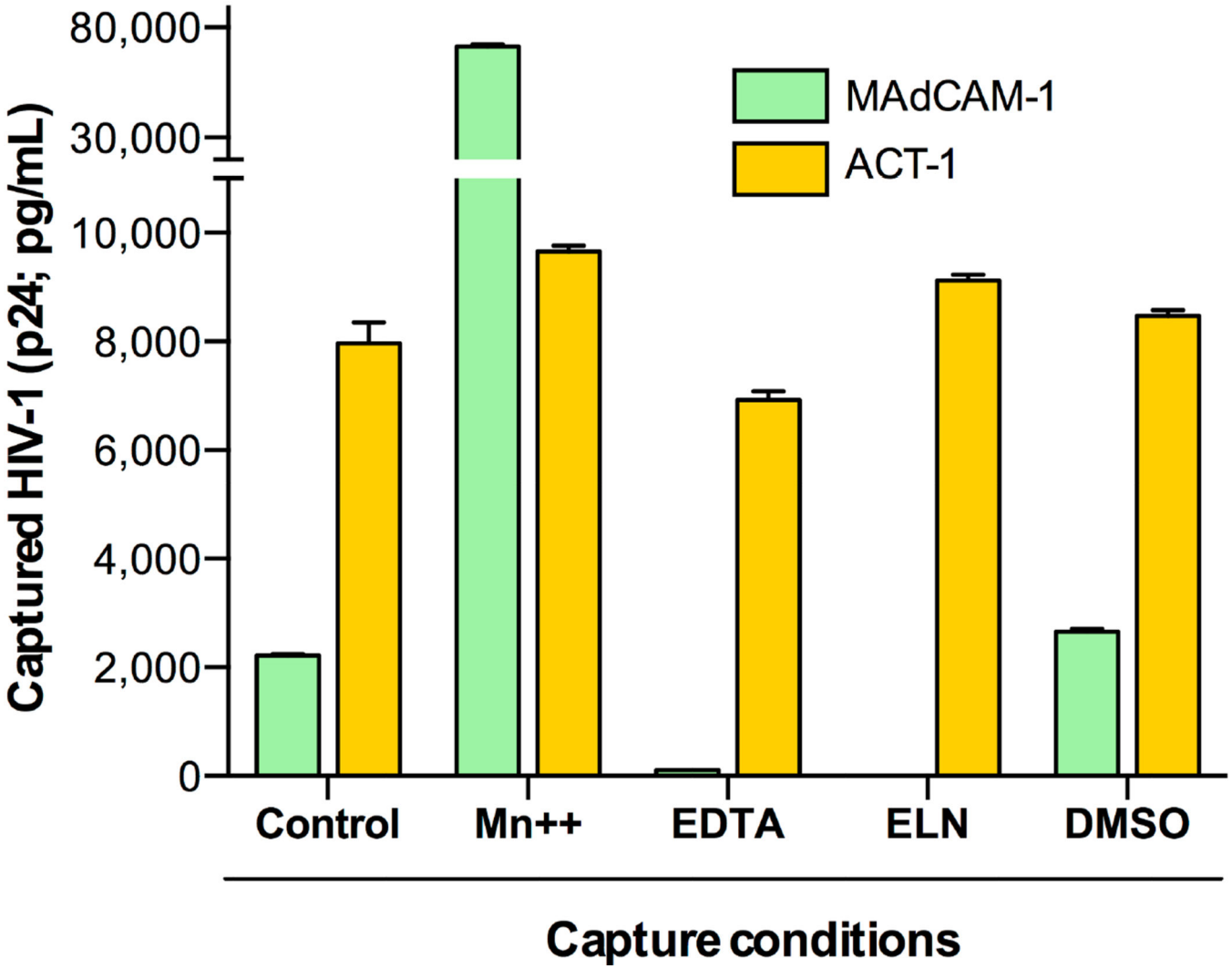

Fig. 3. Virion-incorporated integrin α4β7 is functionally competent

Virion capture assays were performed on the HIV-1 SF162 $\alpha4\beta7_{hi}$ viral stock (produced by RA-treated PBMC) in the presence or absence of functional inhibitors or activators of α4β7, compared to the untreated control condition. Capture with recombinant human MAdCAM-1, which selectively binds to the functionally active integrin, was compared to capture with the anti-α4β7 mAb ACT-1, which binds independently of the integrin activation state. The divalent cation Mn^{++} induces α4β7 to adopt a high-affinity ligand-binding state; the chelating agent EDTA sequesters divalent cations; and the inhibitory peptide mimetic ELN-4757772 (ELN) specifically occludes the MAdCAM-binding site on α4β7, but does not overlap with the ACT-1 epitope. The data represent the mean (±SE) of duplicate samples.

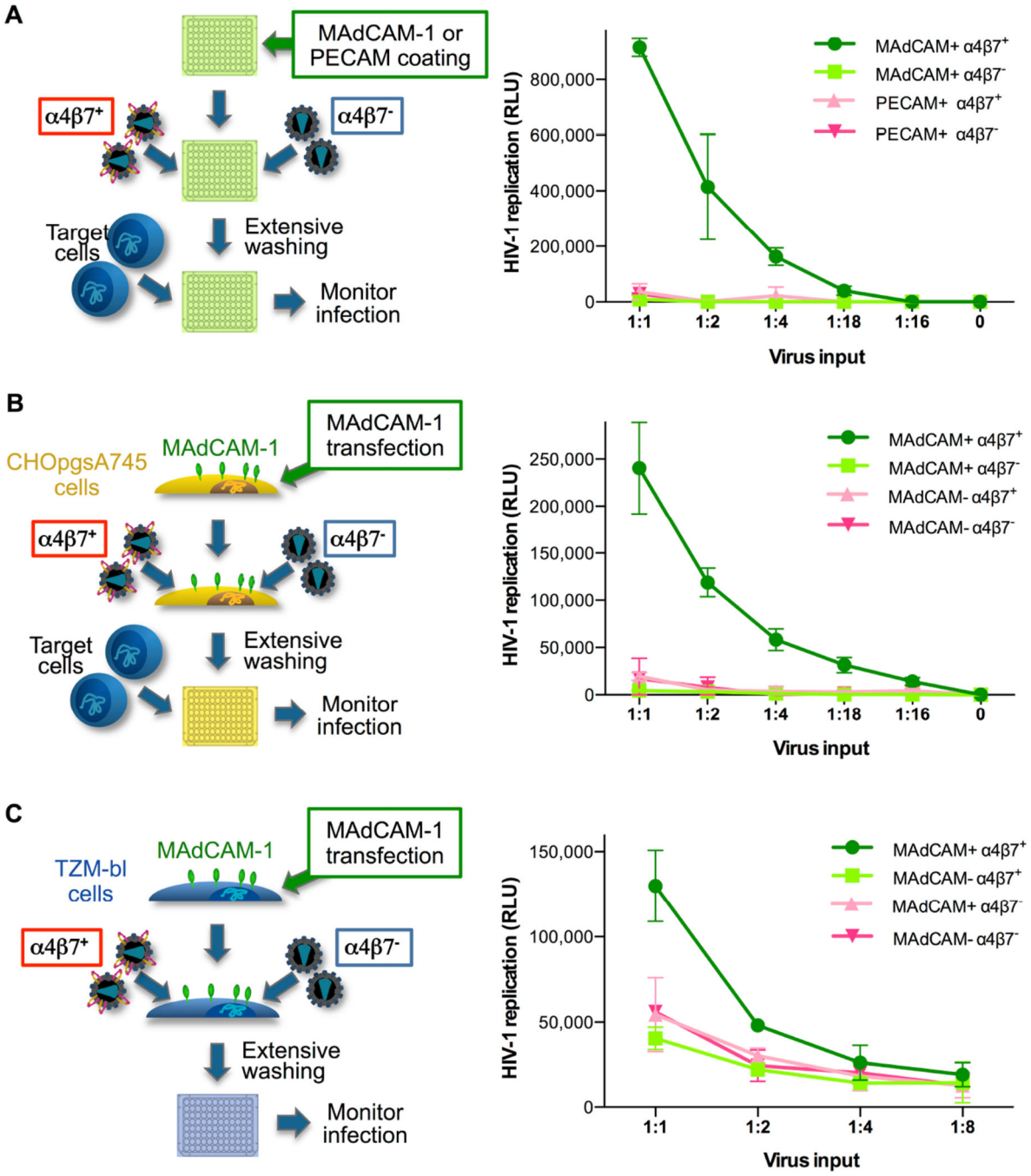

Fig. 4. Incorporation of α4β7 promotes MAdCAM-mediated HIV-1 capture, *trans*-infection of bystander target cells and infection of MAdCAM-expressing target cells

(**A**) HIV-1 virions with incorporated α4β7 were selectively captured by plate-immobilized MAdCAM-1 and transferred to susceptible target cells. Serial dilutions of HIV-1 THRO.18 viral stocks either positive (α4β7^{+}) or negative (α4β7^{-}) for α4β7 were incubated with plastic-coated rhMAdCAM-1 (MAdCAM+, green lines) or an irrelevant integrin ligand (PECAM+, pink lines), washed extensively to remove unbound virus, and overlaid with target cells (TZM-bl), as illustrated in the accompanying cartoon. (**B**) HIV-1 virions with

incorporated α4β7 are selectively captured by MAdCAM-expressing cells, which mediate *trans*-infection of bystander target cells. Serial dilutions of HIV-1 THRO.18 viral stocks either positive ($\alpha4\beta7^{+}$) or negative ($\alpha4\beta7^{-}$) for α4β7 were incubated with MAdCAM-1-expressing cells (MAdCAM+, green lines) or with untransfected control cells (MAdCAM-, pink lines), washed extensively to remove unbound virus, and cocultured with TZM-bl cells. (**C**) HIV-1 virions with incorporated α4β7 infect MAdCAM-expressing susceptible cells more efficiently than $\alpha4\beta7^{-}$ virions. Serial dilutions of HIV-1 BaL pseudoviruses either positive ($\alpha4\beta7^{+}$) or negative ($\alpha4\beta7^{-}$) for α4β7 were incubated with TZM-bl cells transfected to express MAdCAM-1 (MAdCAM+, green) or with untransfected control TZM-bl (MAdCAM-, pink). In all the experiments, HIV-1 infection was assessed by measuring activation of the luciferase reporter gene.

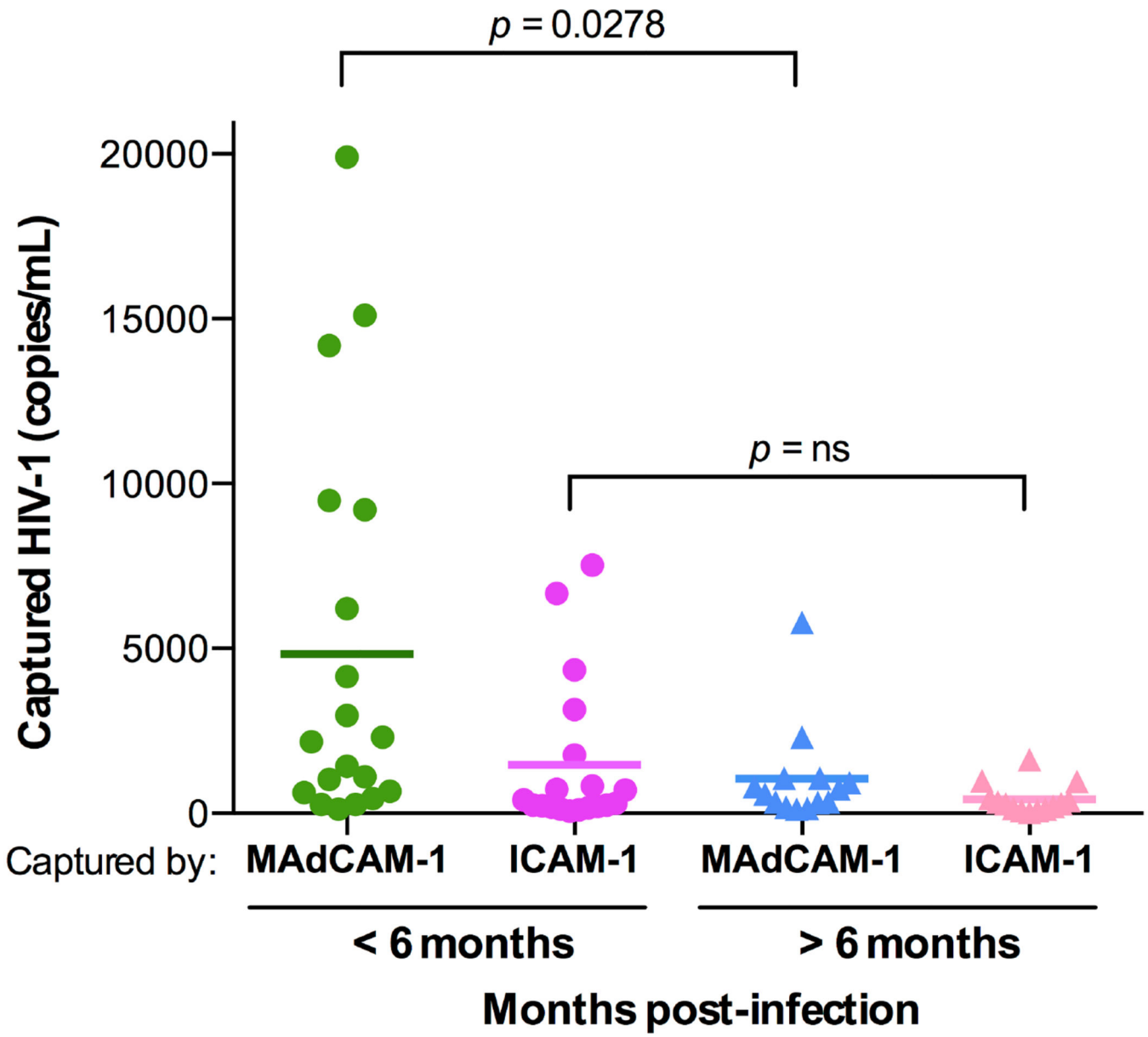

Fig. 5. Integrin α4β7 is incorporated into HIV-1 virions circulating *in vivo* in infected patients

MAdCAM-1$^-$ and ICAM-1-mediated capture of cell-free HIV-1 virions circulating in serum from infected patients. Sera on the left side were obtained during the early stage of HIV-1 infection (0-6 months), while those on the right side were obtained during the chronic phase, after 6 months of primary infection. Due to the limited amount of patient serum available, capture could only be performed with the recombinant α4β7 ligand, MAdCAM-1, which permitted to document the functionality of the incorporated integrin, as well as with ICAM-1, used as a control integrin ligand. Captured virions were quantified by real-time PCR using specific HIV-1 primers and probes on serum-extracted RNA; the results are expressed as viral genome equivalents per mL. Statistical analysis was performed using an unpaired 2-tailed t-test. In addition to the statistical comparisons shown in the figure, the difference between MAdCAM-1$^-$ and ICAM-1-mediated virus capture in the <6-months

group was also statistically significant ($p = 0.0278$ by paired 2-tailed t-test), while no statistical difference was detected in the >6-months group.

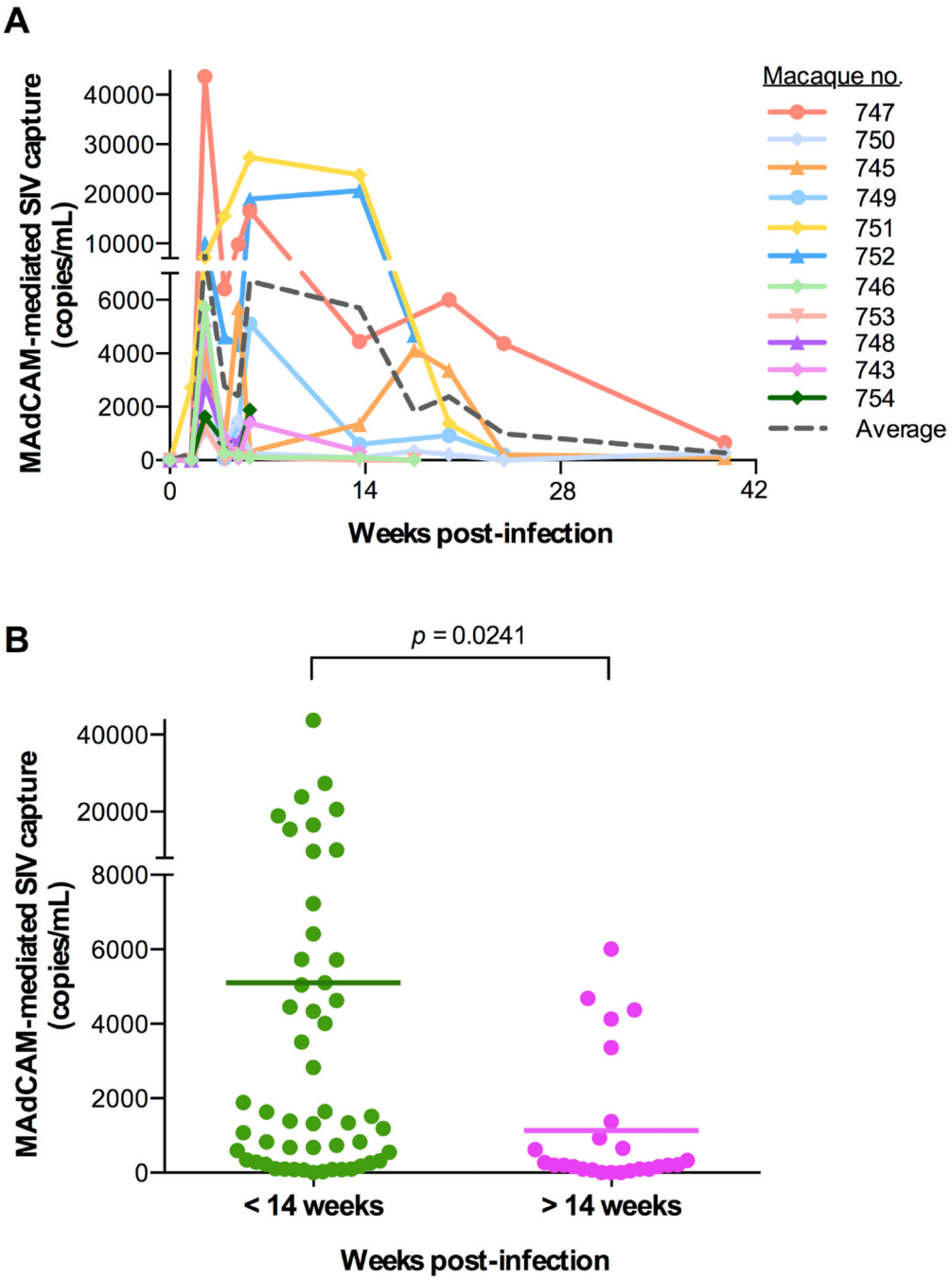

Fig. 6. Integrin α4β7 is incorporated into SIV virions circulating *in vivo* in infected macaques

(**A**) MAdCAM-1-mediated SIV virion capture in plasma samples obtained from 12 macaques experimentally infected with SIVmac239 followed longitudinally during the acute and chronic phases of infection. Captured virions were quantified by real-time PCR using specific SIV primers and probes on plasma-extracted RNA; the results are expressed as viral genome equivalents per mL. (**B**) Statistical comparison showing increased MAdCAM-1-mediated SIV virion capture in plasma samples obtained from infected macaques within the first 14 weeks of infection (acute infection) versus those obtained after 14 weeks of infection

(chronic infection) ($p = 0.0241$). Statistical analysis was performed using an unpaired 2-tailed t-test.

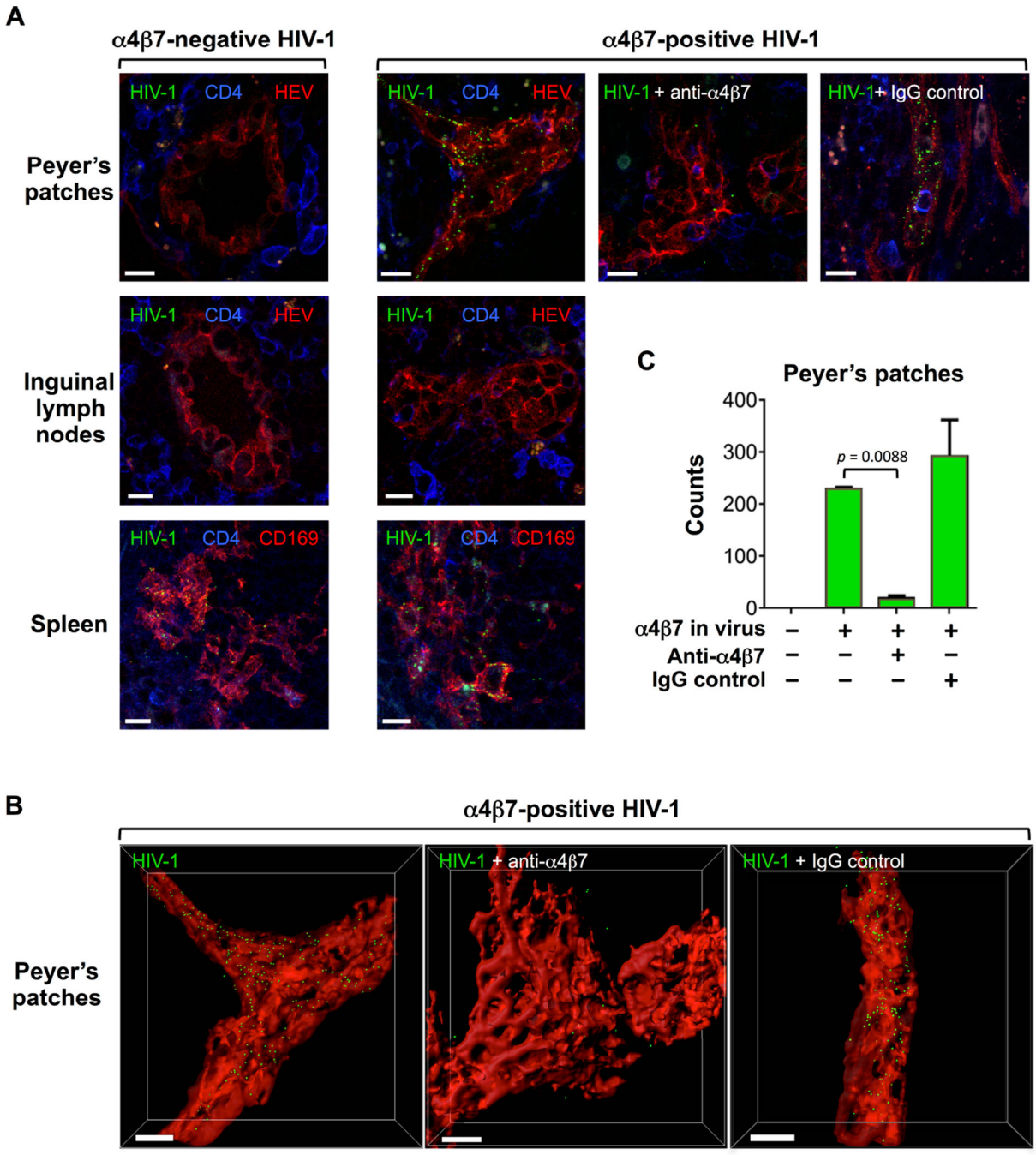

Fig. 7. Incorporation of α4β7 promotes HIV-1 gut homing *in vivo*

(**A**) Thick-section images of HIV-1 uptake *in vivo* by Peyer's patches, inguinal lymph nodes and spleen of mice injected with green fluorescent $\alpha4\beta7^{-}$ (left column) and $\alpha4\beta7^{+}$ (right 3 columns) HIV-1 virions. Normalized viral stocks of reverse transcriptase-deficient fluorescent HIV-1 (NL4.3 Gag EGFP) either negative ($\alpha4\beta7^{-}$) or positive ($\alpha4\beta7^{+}$) for α4β7 incorporation were inoculated into the tail base of C57BL/6 mice. After 45 minutes, the animals were euthanized, and the indicated organs were extracted and analyzed by confocal microscopy. The three panels in the left column show $\alpha4\beta7^{-}$ virus; all the panels on the

right columns show $\alpha4\beta7^+$ virus. A primatized anti-$\alpha4\beta7$ mAb (ACT-1) or an isotype-control macaque mAb were pre-incubated with the viral stocks prior to inoculation. The sections were stained with anti-CD4 (blue) or anti-CD169 and anti-PNAd (red) antibodies, as indicated; PNAd staining specifically labels high endothelial venules (HEV) in Peyer's patches. $\alpha4\beta7^+$ virions (green) were selectively and specifically captured by HEV in Peyer's patches. In spleen tissue, both viruses (green) were visible on $CD169^+$ (red) marginal zone macrophages, while no virion uptake was detected in inguinal lymph nodes. Scale bars denote 5 μm. (**B**) Three-dimensional reconstructions of HEV (red) and HIV-1 virions (green spots) of the three images shown in panel **A**, top row, right columns, generated with the surface and spot functions of the Imaris program. Scale bars denote 5 μm. (**C**) Quantification of $\alpha4\beta7^+$ and $\alpha4\beta7^-$ HIV-1 virion uptake in Peyer's patches, as assessed in the images shown in panel **A**, top row. Statistical analysis of virus uptake in the presence of $anti^-$ $\alpha4\beta7$ mAb vs. control mAb was performed by paired 2-tailed t-test.

Table 1

Incorporation of α4β7 and ICAM-1 in a panel of clinical and laboratory HIV-1 and SIV isolates of different clade and coreceptor usage phenotypes grown in activated primary human PBMC. All the clinical isolates were minimally passaged *in vitro*. The level of virion incorporation was evaluated by measuring the amount of captured $p24_{Gag}$ (or $p27_{Gag}$ for SIV) antigen by immunomagnetic beads armed with anti-ICAM-1/CD54 or anti-α4β7 monoclonal antibodies, and was color-coded in different shades of red (darker to lighter: >1000; 400–1000; 100–400; 0–100 pg/mL).

Virus	Strain	Clade	Coreceptor usage	Virion incorporation*	
				ICAM-1	α4β7
HIV-1	92UG037	A	R5	9	406
HIV-1	BaL	B	R5	275	768
HIV-1	ADA	B	R5	305	451
HIV-1	JRFL	B	R5	11	1379
HIV-1	IIIB	B	X4	64	1385
HIV-1	07USLD	B	X4	83	658
HIV-1	07USLR	B	X4	50	1373
HIV-1	92HT599	B	R5×4	42	830
HIV-1	93UG065	D	X4	414	719
HIV-1	93TH057	E	R5	0	457
HIV-1	CMU06	E	X4	0	233
HIV-1	97BR019	F	R5×4	0	733
SIV	smE660.307	n.a.	R5	200	508
SIV	mac251.745	n.a.	R5	235	1499

*Amount of $p24_{Gag}$ (or $p27_{Gag}$) antigen (in pg/mL) captured from normalized input virus.